materials

MDPI

Communication

Investigation of Charging Efficiency of a Lithium-ion Capacitor during Galvanostatic Charging Method

Shunji Nakata

Department of Electronic Engineering and Computer Science, Faculty of Engineering, Kindai University, Takaya, Higashi-Hiroshima 739-2116, Japan; nakata@hiro.kindai.ac.jp

Received: 7 August 2019; Accepted: 24 September 2019; Published: 29 September 2019

Abstract: The charging efficiency of a lithium-ion capacitor (LIC) is an important problem. Until now, due to the stepwise charging method, the charging efficiency of 95.5% has been realized. However, the problem is that the issue of what level the charging efficiency can be increased to, is yet to be well investigated. In this article, the problem is investigated under the galvanostatic charging condition. The charging efficiency is measured as a function of the charging current. As a result, it can be more than 99.5% when the charging is quasi-static, in other words, an adiabatic process is realized. Next, the problem of how much energy can be taken out from the energy-stored capacitor is investigated with a load resistor circuit. It is clarified that the discharging energy from the capacitor is equal to the stored energy in the case when a load resistor is used and the discharging is quasi-static. It is confirmed that LICs are suitable for use as energy storage devices.

Keywords: charging efficiency; lithium-ion capacitor; adiabatic charging; energy dissipation

1. Introduction

Recently, the energy storage of renewable energy is an important problem. To store energy, supercapacitors are considered to play an important role. In particular, lithium-ion capacitors (LICs) have attractive characteristics [1–6]. The LICs have many advantages over lithium-ion batteries. The power density is 10 times larger and the operating temperature has a wider range [1]. The cycle lifetime of LICs is 1,000,000 cycles [2], while that of lithium-ion batteries is about 2000 cycles [7,8]. Another important point is that LICs are much safer than lithium-ion batteries. On the other hand, there is a drawback, such as energy density. The energy density of commercial LICs is 13 Wh/kg [9], while that of lithium-ion batteries is 100 Wh/kg [1], i.e., LICs are 13% that of the batteries. However, when there is a large space, it is not a serious problem. These advantageous characteristics make LICs very suitable for storing energy from renewable resources.

Dissipationless adiabatic charging of a capacitor has been researched [10–30]. Recently, a stepwise charging and discharging circuit has been proposed, which does not need a shunt resistor for detecting the current [23,26,27,29]. The proposed circuit is composed of switching transistors and an inductor. By changing the duty ratio of transistors digitally, stepwise charging is realized, which in turn, means the realization of adiabatic charging. The digital control of duty ratio is achieved by a microprocessor (PIC16F627A) (Microchip Technology, Chandler, AZ, USA), which outputs the Pulse Width Modulation (PWM) signal [27,29]. It was clarified experimentally that the charging efficiency is 95.5% during charging and also discharging. However, the question remains—to what level can the charging efficiency be increased? In this article, the charging efficiency of the LIC is investigated with the constant current or galvanostatic charging method and investigated as a function of the charging current. The paper is organized as follows: Section 2 gives the charging measurement system and experimental results, Section 3 presents the discharging measurement system from the energy-stored

capacitor and the experimental results, Section 4 discusses the experimental results. The conclusion is given in Section 5.

2. Charging Experiment

Figure 1 shows the measurement system in this experiment. The power supply is Agilent Technologies U8001A (Agilent Technologies, Inc., Santa Clara, CA, USA). Three multimeters are used for measuring the output voltage of power supply V_P, the current flowing from the power supply into the capacitor I_1, and the capacitor voltage V_C. To realize galvanostatic charging, the maximum output current is set on U8001A. The LIC in this experiment is LIC1235RS3R8406 (Taiyo Yuden Co., Ltd., Tokyo, Japan). The capacitance is 40 F. The rated current of the capacitor is 2 A. The energy density of the LIC is 10 Wh/kg. The minimum and maximum operating voltages are 2.2 and 3.8 V. In this experiment, for the sufficient voltage margin from the voltage limit, the initial and final capacitor voltages during charging are set to 2.38 and 3.60 V, respectively. In the measurement, the timing of data capture is from the beginning, 2.38 V, to the ending point, 3.6 V.

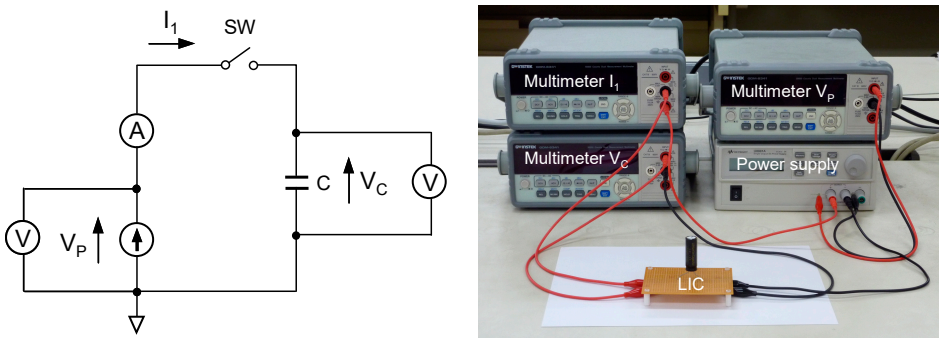

Figure 1. (**a**) Measurement system used when galvanostatic charging is performed. I_1 is the charging current from the power supply to the lithium-ion capacitator (LIC); (**b**) photograph of the measurement system.

First, the maximum voltage and the maximum charging current are set to 3.6 V and 0.09 A on the power supply, respectively. Figure 2a shows I_1. When t = 11 s, the power supply and the capacitor are connected. The current is increased from 0 to 0.09 A. When t = 520s, the capacitor voltage is close to 3.6 V. Then, the power supply becomes a constant voltage charging mode, and the current decreases rapidly from 0.09 A. The V_C is shown in Figure 2b. The value reaches 3.60 V at t = 620 s, finally. Figure 3a shows V_P. In the beginning, the value is 3.6 V and is decreased rapidly to 2.4 V at t = 11 s after the power supply and capacitor are connected. It then reaches to 3.60 V at t = 520 s.

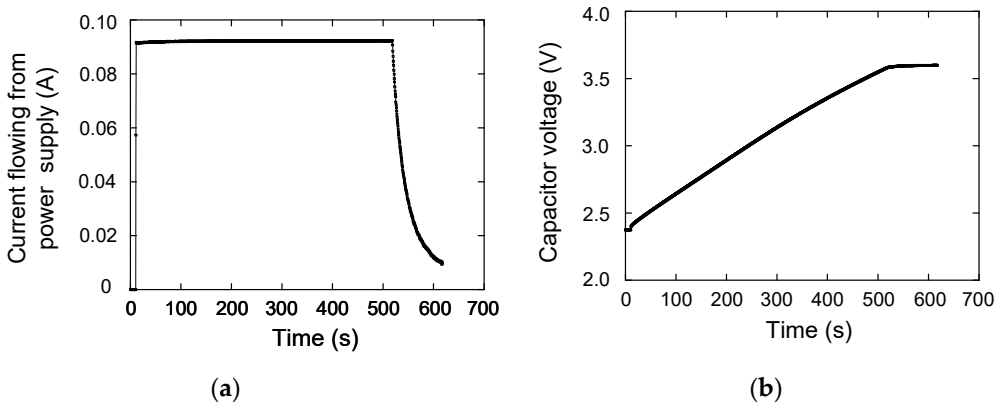

Figure 2. (**a**) Capacitor charging current as a function of time; (**b**) capacitor voltage as a function of time.

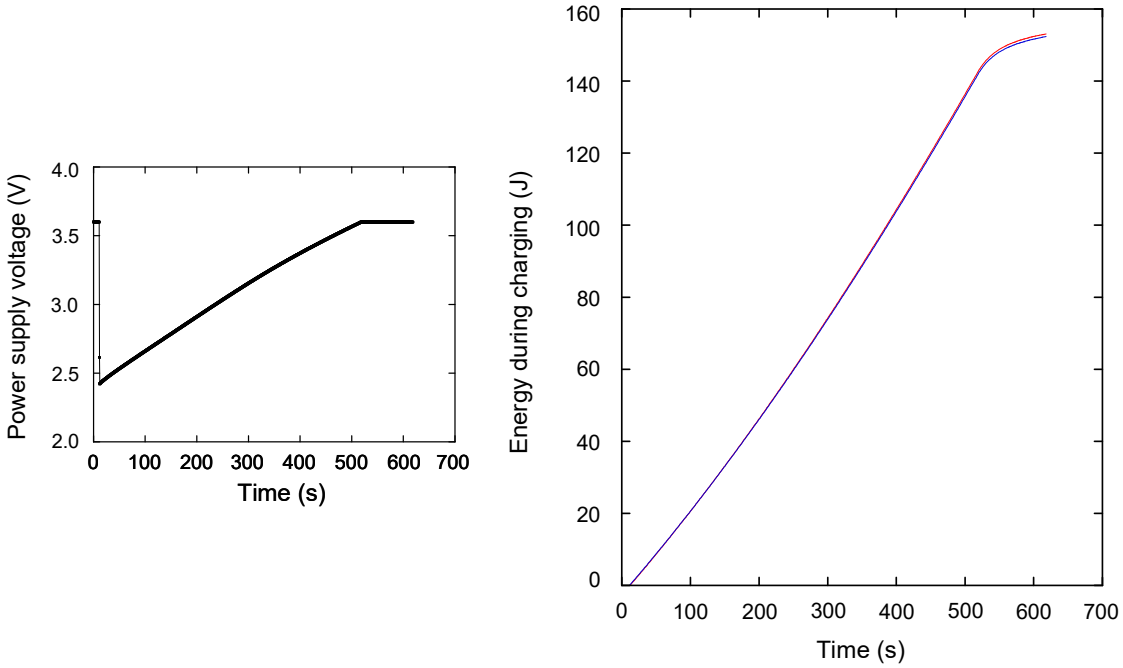

(**a**) (**b**)

Figure 3. (**a**) Power supply output voltage as a function of time; (**b**) work done by the power supply (red line) and stored energy of the capacitor (blue line).

Here, the C-rate of the charging current is considered. The capacity of the LIC is calculated to be 40 F × (3.8 V−2.2 V) = 64 C. Therefore, a 1 C-rate is 64 C/3600 s = 0.0178 A. Then, 0.09 A is equal to a 5.1 C-rate.

From these measurement results, the work done by the power supply E_P is calculated as $E_P = \int I_1 V_P \, dt$. On the other hand, the stored energy in the capacitor during charging E_{C1} is calculated as $E_{C1} = \int I_1 V_C \, dt$. The suffix 1 means it is related to the charging, and the suffix 2 is used for the discharging process, which is discussed in the next section. The E_P and E_{C1} are shown in Figure 3b as the red and blue lines, respectively. These are almost consistent, which means the charging efficiency η is almost 1. At t = 620 s, E_P and E_{C1} are 153.11 and 152.33 J, respectively, so η is calculated to be E_{C1}/E_P = 0.995. The energy loss is considered to be the energy dissipation in wire resistance. This wire resistance is calculated from the experiment, and also the energy dissipation is calculated. Figure 4a shows the wire resistance R_W as a function of time, which is calculated from $(V_P - V_C)/I_1$. The average value during galvanostatic charging is 0.21 Ω. The energy dissipation can be calculated by $E_{diss} = \int R_W {I_1}^2 \, dt$, and it is shown in Figure 4b. The value reaches to 0.92 J at t = 620 s, which is almost consistent with the difference between E_P and E_{C1}, 0.78 J.

Figure 5a shows the charging efficiency as a function of the charging current. The charging current values are 0.03, 0.09, 0.4, 0.8, 1.2, 1.6, and 2.0 A. The rated current is 2.0 A in this capacitor, so the experiment over 2.0 A was not performed. These currents correspond to a 1.7, 5.1, 22.5, 45.0, 67.5, 90.0, and 112.5 C-rate, respectively. The charging efficiencies to those current values are 99.8%, 99.5%, 97.9%, 96.2%, 94.7%, 93.3%, and 92.0%, respectively. For a profound understanding, the charging efficiency during constant voltage charging is considered. In the experiment, V_C is changed from 2.4 to 3.6 V. Therefore, for easy calculation, the initial and final voltages are set to $2V/3$ and V, respectively, where V is the constant power supply voltage. The charge amount difference ΔQ is $CV/3$, where C is the capacitance. So the work done by the power supply W is $W = \Delta Q \times V = CV^2/3$. On the other hand, electrostatic energy difference during charging ΔE_1 is written as $\Delta E_1 = C/2 \times \{V^2 - (2V/3)^2\} = 5/18 \cdot CV^2$. Therefore, the charging efficiency is calculated to be $\eta = \Delta E_1/W$ = 83.3%, which is shown in Figure 5b

as a solid line. For comparison, the previous charging efficiencies are also plotted. If the galvanostatic charging current increased over 2 A, the charging efficiency would approach to 83.3%.

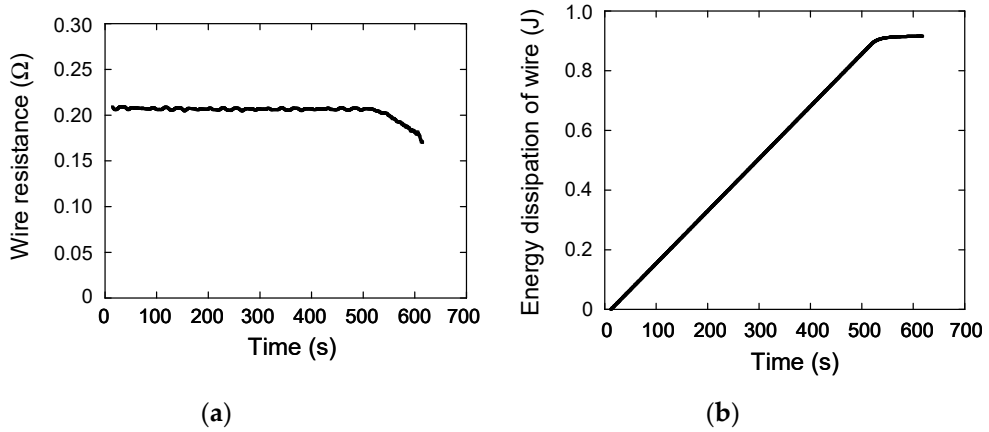

(**a**) (**b**)

Figure 4. (**a**) Wire resistance as a function of time; (**b**) energy dissipation of the wire as a function of time.

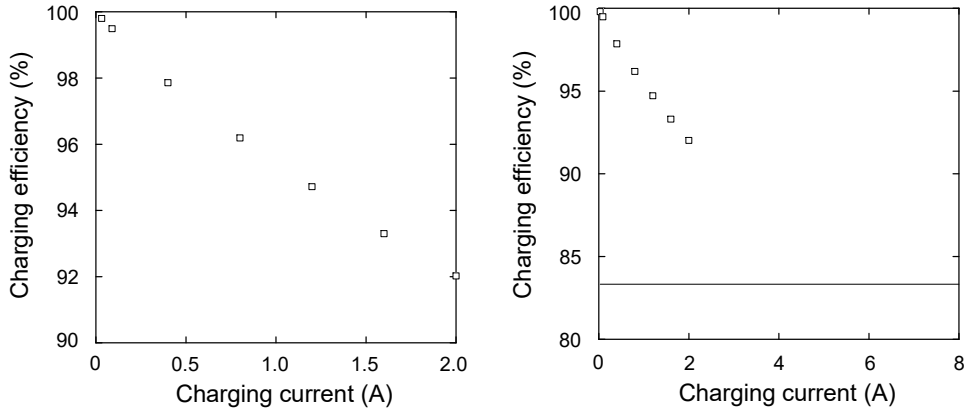

(**a**) (**b**)

Figure 5. (**a**) Charging efficiency as a function of current; (**b**) comparison between galvanostatic charging and constant voltage charging (solid line).

3. Discharging Experiment

In the previous section, the stored energy during charging is discussed. Here, the problem of how much energy can be taken out from the energy-stored capacitor is discussed. The discharging experimental system is shown in Figure 6. The discharging current flows from the capacitor to a load resistor. The capacitor voltage, the current flowing from the capacitor I_2, and the load resistor voltage V_R are measured with three multimeters. The nominal load resistance is 100 Ω. The V_C during discharging is shown in Figure 7a. The initial and final voltages are 3.60 and 2.38 V, respectively. After 1720 s, V_C reaches to 2.38 V, which is the same as the initial voltage when charging is performed. The I_2 is shown in Figure 7b. When $t = 0$, a switch is open and current does not flow. Therefore, I_2 is zero. When $t = 10$ s, a switch is closed and current flows. Then, I_2 increases rapidly to 0.036 A. When $t = 1720$ s, the switch is open and I_2 becomes 0 A. Here, the discharging energy E_{C2} is calculated as $E_{C2} = \int I_2 V_C \, dt$. The calculated result is shown in Figure 8. When $t = 1720$ s, E_{C2} becomes 152.62 J, which is consistent with the value of E_{C1}, 152.33 J, and the difference between them is only 0.19%.

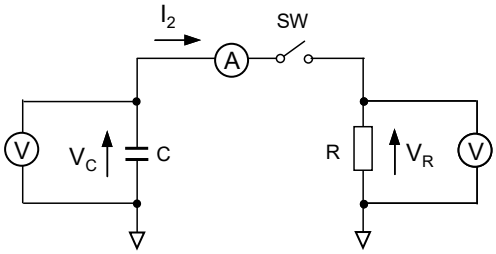

Figure 6. Measurement system when discharging is performed. I_2 is the discharging current from the energy-stored capacitor to a load resistor.

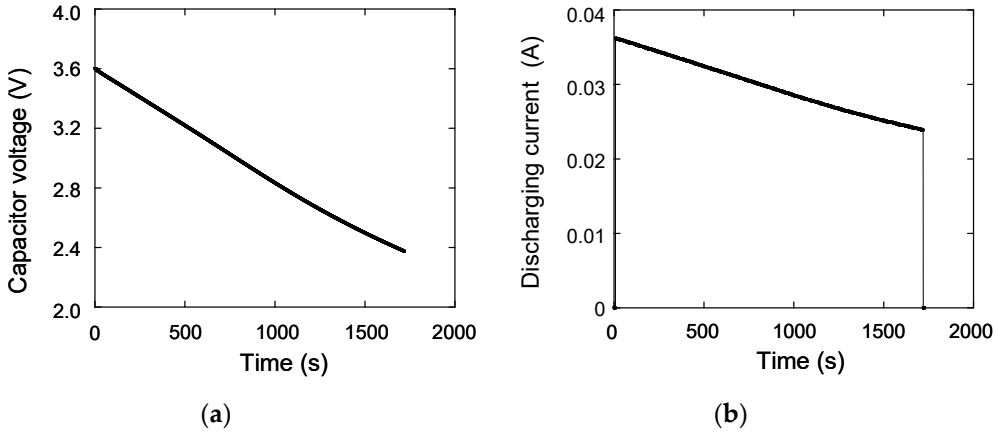

Figure 7. (**a**) Capacitor voltage as a function of time during discharging; (**b**) discharging current as a function of time.

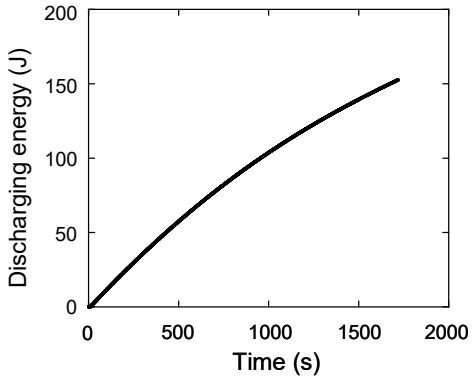

Figure 8. Discharging energy taken out from a capacitor.

Next, the discharging energy is investigated from the viewpoint of the Joule heat of the resistor in the circuit, which is composed of the load resistor and the wire one. The actual load resistance R_L is calculated as V_R/I_2. The V_R during discharging is shown in Figure 9a. When t = 0, a switch is open and current does not flow. Therefore, V_R is zero. When t = 10 s, current flows and V_R increases to 3.6 V, which is almost consistent with V_C. When t = 1720 s, a switch is open and current does not flow. Then, V_R becomes 0 V. Using V_R, V_R/I_2 is calculated, which is shown in Figure 9b. The average value is 98.8 Ω, which is consistent with the nominal value.

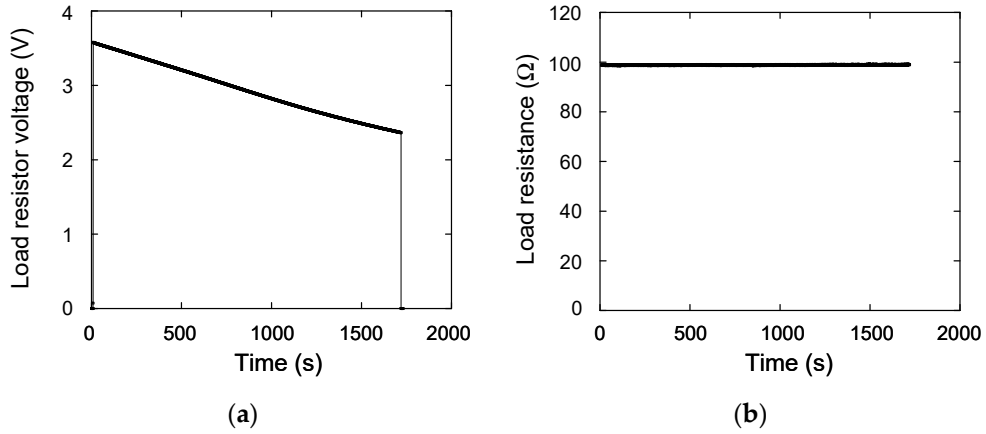

Figure 9. (**a**) Load resistor voltage as a function of time; (**b**) load resistance as a function of time.

Using the wire terminal voltage difference $V_C - V_R$, the wire resistance R_W is calculated as $(V_C - V_R)/I_2$. The value of $V_C - V_R$ is shown in Figure 10a. The calculated value of R_W is shown in Figure 10b. The average value is 0.383 Ω. Then, the energy dissipation due to the Joule heat is calculated as $E_{diss} = \int (R_L + R_W)\, {I_2}^2\, dt$. The result is shown in Figure 11. At t = 1720 s, E_{diss} reaches to 152.41 J. This value is consistent with the previously calculated value of E_{C1} and E_{C2}.

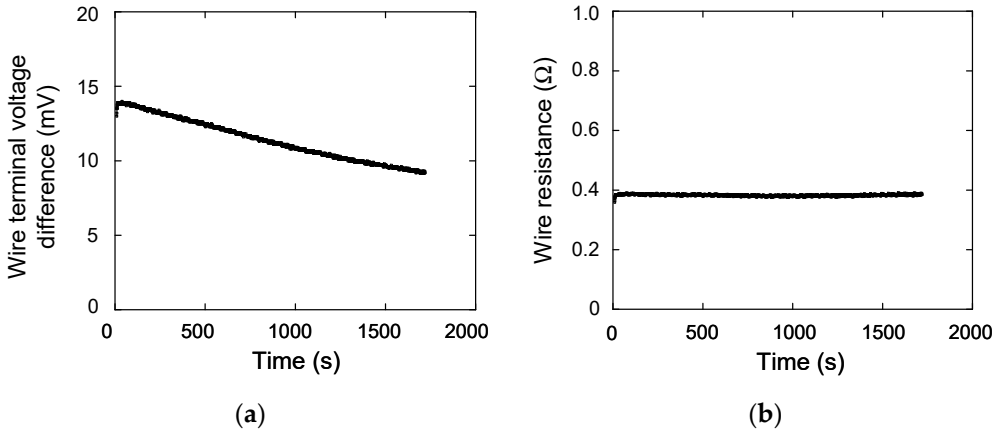

Figure 10. (**a**) Wire terminal voltage difference as a function of time; (**b**) wire resistance as a function of time.

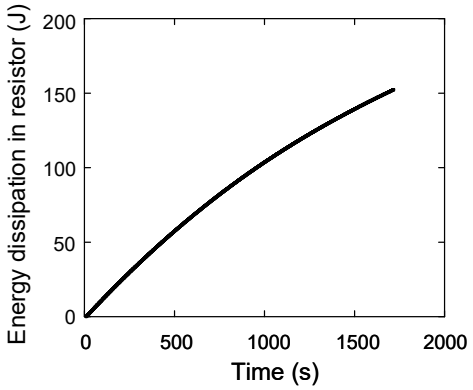

Figure 11. Energy dissipation caused at the resistor.

4. Discussion

In the energy storage device, the coulombic efficiency is discussed, which is defined as C_d/C_c, where C_d is the discharging capacity and C_c is the charging capacity [31]. In the voltage range from 2.38 to 3.6 V in this experiment, C_c and C_d are almost the same and they are 50.46 and 50.45 C, respectively. The coulombic efficiency is calculated to be 0.9996.

Here, the Peukert effect is considered. It is written as $C_{n1} = C_n(I_n/I_{n1})^{k-1}$, where I_n is the manufacturer-specified discharge current, C_n is the rated capacity at I_n, I_{n1} is a different discharge current, C_{n1} is the available capacity at I_{n1}, and k is the Peukert coefficient [32]. From this equation, when I_{n1} becomes large, C_{n1} becomes small. This equation is applied not only to lead-acid and Li-ion batteries but also to Electric Double-Layer Capacitors (EDLCs) [33] and LICs [34–36] in the wide current range.

Then, the case where I_2 becomes large is considered. The E_{C2} is rewritten as follows: $E_{C2} = \int I_2 V_C \mathrm{d}t = I_2 \int V_C \mathrm{d}t = V_{av} I_2 T$, where T is the discharging time and V_{av} is the average voltage defined as $\int V_C \mathrm{d}t/T$. If I_2 is large, the capacity $I_2 T$ becomes small due to the Peukert effect. Therefore, E_{C2} becomes small, which means the total efficiency of charging and discharging E_{C2}/E_P decreases. For increasing the total efficiency, the discharging current should be small, in other words, an adiabatic process has to be performed.

Regarding the energy efficiency of LICs, there are the following literature references. Reference [37] describes the efficiency of the LIC-based distributed uninterruptible power supply (UPS system. It shows that the experimental efficiency of the LIC with 3300 F is about 95% when the LIC module voltage changes from 6 to 7 V.

Reference [38] describes the efficiency of LICs (JM Energy) is 97% from simulation results. Reference [39] shows the efficiency of LICs is 80% from experimental results.

In this experiment, it is clarified that the charging efficiency changes from 92% to 99.8% systematically as a function of galvanostatic current.

5. Conclusions

For energy storage of renewable resources, LICs are attractive for the lifetime and safety in comparison with lithium-ion batteries. Regarding the energy density, the commercial LICs have a large energy density (13 Wh/kg) [9], which is close and comparable to that of lead-acid batteries. Therefore, LICs are promising for energy storage. Until now, the charging efficiency of the LIC was investigated with a stepwise charging circuit, and it was 95.5%. In this article, this charging efficiency is investigated in detail with the galvanostatic method. As a result, in the adiabatic charging, the charging efficiency is more than 99.5%. The energy dissipation is due to the Joule heat of the wire resistance. Next, how much energy in charging can be taken out during discharging was investigated. The experiment shows the discharging energy is equal to the energy during charging. This is due to no Joule heat energy dissipation for the adiabatic process and no leakage current for the LIC characteristic. From the result, the LIC causes no energy dissipation in the adiabatic process, and it is useful for energy storage devices.

Author Contributions: Conceptualization, Investigation, Formal analysis, Writing (Review and Editing), and Supervision, S.N.

Funding: This research received no external funding.

Conflicts of Interest: The authors declare no conflicts of interest.

References

1. What is LIC. Available online: https://www.jmenergy.co.jp/en/lithium_ion_capacitor/ (accessed on 25 September 2019).
2. Product Information. Available online: https://www.jmenergy.co.jp/en/product/cell/can_testresults/ (accessed on 25 September 2019).

3. Liu, C.; Ren, Q.-Q.; Zhang, S.-W.; Yin, B.-S.; Que, L.-F.; Zhao, L.; Sui, X.-L.; Yu, F.-D.; Li, X.; Gu, D.-M.; et al. High energy and power lithium-ion capacitors based on Mn3O4/3D-graphene as anode and activated polyaniline-derived carbon nanorods as cathode. *Chem. Eng. J.* **2019**, *370*, 1485–1492. [CrossRef]
4. Huang, J.-L.; Fan, L.-Q.; Gu, Y.; Geng, C.-L.; Luo, H.; Huang, Y.-F.; Lin, J.-M.; Wu, J.-H. One-step solvothermal synthesis of high-capacity Fe3O4/reduced graphene oxide composite for use in Li-ion capacitor. *J. Alloys Compd.* **2019**, *788*, 1119–1126. [CrossRef]
5. Sennu, P.; Arun, N.; Madhavi, S.; Aravindan, V.; Lee, Y.-S. All carbon based high energy lithium-ion capacitors from biomass: The role of crystallinity. *J. Power Sources* **2019**, *414*, 96–102. [CrossRef]
6. Boltersdorf, J.; Delp, S.A.; Yan, J.; Cao, B.; Zheng, J.P.; Jow, T.R.; Read, J.A. Electrochemical performance of lithium-ion capacitors evaluated under high temperature and high voltage stress using redox stable electrolytes and additives. *J. Power Sources* **2018**, *373*, 20–30. [CrossRef]
7. Sinkaram, C.; Rajakumar, K.; Asirvadam, V. Modeling battery management system using the lithium-ion battery. In Proceedings of the 2012 IEEE International Conference on Control System, Computing and Engineering, Penang, Malaysia, 23–25 November 2012; pp. 50–55.
8. Podder, S.; Khan, M.Z.R. Comparison of lead acid and li-ion battery in solar home system of Bangladesh. In Proceedings of the 2016 5th International Conference on Informatics, Electronics and Vision (ICIEV), Dhaka, Bangladesh, 13–14 May 2016; pp. 434–438.
9. ULTIMO Lithium Ion Capacitor Prismatic Cells. Available online: https://www.jsrmicro.be/emerging-technologies/lithium-ion-capacitor/products/ultimo-lithium-ion-capacitor-prismatic-cells (accessed on 25 September 2019).
10. Svensson, L.J.; Koller, J.G. Driving a capacitive load without dissipating fCV^2. In Proceedings of the 1994 IEEE Symposium on Low Power Electronics, San Diego, CA, USA, 10–12 October 1994; pp. 100–101.
11. Athas, W.C.; Svensson, L.J.; Koller, J.G.; Tzartzanis, N.; Chou, E.Y.-C. Low-power digital systems based on adiabatic-switching principles. *IEEE Trans. Very Large Scale Integr. (VLSI) Syst.* **1994**, *2*, 398–407. [CrossRef]
12. Moon, Y.; Jeong, D.-K. An efficient charge recovery logic circuit. *IEEE J. Solid-State Circuits* **1996**, *31*, 514–522. [CrossRef]
13. Nakata, S.; Douseki, T.; Kado, Y.; Yamada, J. A Low Power Multiplier Using Adiabatic Charging Binary Decision Diagram Circuit. *Jpn. J. Appl. Phys.* **2000**, *39*, 2305–2311. [CrossRef]
14. Kim, S.; Papaefthymiou, M.C. True single-phase adiabatic circuitry. *IEEE Trans. Very Large Scale Integr. (VLSI) Syst.* **2001**, *9*, 52–63.
15. Kim, S.; Ziesler, C.H.; Papaefthymiou, M.C. A true single-phase energy-recovery multiplier. *IEEE Trans. Very Large Scale Integr. (VLSI) Syst.* **2003**, *11*, 194–207.
16. Nakata, S. Adiabatic charging reversible logic using a switched capacitor regenerator. *IEICE Trans. Electron* **2004**, *E87-C*, 1837–1846.
17. Hwang, M.-E.; Raychowdhury, A.; Roy, K. Energy-recovery techniques to reduce on-chip power density in molecular nanotechnologies. *IEEE Trans. Circuits Syst. I: Regul. Pap.* **2005**, *52*, 1580–1589. [CrossRef]
18. Chan, S.C.; Shepard, K.L.; Restle, P.J. Distributed Differential Oscillators for Global Clock Networks. *IEEE J. Solid-State Circuits* **2006**, *41*, 2083–2094. [CrossRef]
19. Keung, K.-M.; Manne, V.; Tyagi, A. A Novel Charge Recycling Design Scheme Based on Adiabatic Charge Pump. *IEEE Trans. Very Large Scale Integr. (VLSI) Syst.* **2007**, *15*, 733–745. [CrossRef]
20. van Elzakker, M.; van Tuijl, E.; Geraedts, P.; Schinkel, D.; Klumperink, E.; Nauta, B. A 1.9 μW 4.4fJ/conversion-step 10b 1MS/s charge-redistribution ADC. In Proceedings of the 2008 IEEE International Solid-State Circuits Conference–Digest of Technical Papers, San Francisco, CA, USA, 3–7 February 2008; IEEE: Piscataway, NJ, USA, 2008; pp. 244–245.
21. Nakata, S. Stability of adiabatic circuit using asymmetric 1D-capacitor array between the power supply and ground. *IEICE Electron. Express* **2007**, *4*, 165–171. [CrossRef]
22. Chernichenko, D.; Kushnerov, A.; Ben-Yaakov, S. Adiabatic charging of capacitors by Switched Capacitor Converters with multiple target voltages. In Proceedings of the 2012 IEEE 27th Convention of Electrical and Electronics Engineers in Israel, Eilat, Israel, 14–17 November 2012; pp. 1–4.
23. Nakata, S.; Makino, H.; Hosokawa, J.; Yoshimura, T.; Iwade, S.; Matsuda, Y. Energy Efficient Stepwise Charging of a Capacitor Using a DC-DC Converter With Consecutive Changes of its Duty Ratio. *IEEE Trans. Circuits Syst. I: Regul. Pap.* **2014**, *61*, 2194–2203. [CrossRef]

24. Raghav, H.S.; Bartlett, V.A.; Kale, I. Energy efficiency of 2-step charging power-clock for adiabatic logic. In Proceedings of the PATMOS 2016-The 26th International Workshop on Power And Timing Modeling, Optimization and Simulation, Bremen, Germany, 21–23 September 2016; pp. 176–182.
25. Khorami, A.; Sharifkhani, M. An efficient fast switching procedure for stepwise capacitor chargers. *IEEE Trans.Very Large Scale Integr. (VLSI) Syst.* **2017**, *25*, 705–713. [CrossRef]
26. Nakata, S.; Ono, M.; Sakitani, M. An adiabatic circuit with consecutive changes of the duty ratio of the switching transistor using a microprocessor. *J. Circuits Syst. Comput.* **2017**, *26*, 1750007/1–15. [CrossRef]
27. Nakata, S. An adiabatic charging reversible circuit with stepwise voltage control method using a microprocessor. *Results in Phys.* **2017**, *7*, 2976–2978. [CrossRef]
28. Lee, M.; Yang, J.; Park, M.J.; Jung, S.Y.; Kim, J. Design and analysis of energy-efficient single-pulse piezoelectric energy harvester and power management IC for battery-free wireless remote switch applications. *IEEE Trans. Circuits Syst. I: Reg. Pap.* **2018**, *65*, 366–379. [CrossRef]
29. Nakata, S. Characteristic of an adiabatic charging reversible circuit with a Lithium ion capacitor as an energy storage device. *Results in Phys.* **2018**, *10*, 964–966. [CrossRef]
30. Shah, S.A.A.; Arslan, S.; Kim, H. A Reconfigurable Voltage Converter With Split-Capacitor Charging and Energy Recycling for Ultra-Low-Power Applications. *IEEE Access* **2018**, *6*, 68311–68323. [CrossRef]
31. Yang, F.; Wang, D.; Zhao, Y.; Tsui, K.-L.; Bae, S.J. A study of the relationship between coulombic efficiency and capacity degradation of commercial lithium-ion batteries. *Energy* **2018**, *145*, 486–495. [CrossRef]
32. Doerffel, D.; Abu Sharkh, S. A critical review of using the Peukert equation for determining the remaining capacity of lead-acid and lithium-ion batteries. *J. Power Sources* **2006**, *155*, 395–400. [CrossRef]
33. Yang, H. A Study of Peukert's Law for Supercapacitor Discharge Time Prediction. In Proceedings of the IEEE Power and Energy Society General Meeting (PESGM), Portland, OR, USA, 5–10 August 2018; pp. 1–5.
34. Omar, N.; Ronsmans, J.; Firozu, Y.; Monem, M.A.; Samba, A.; Gualous, H.; Hegazy, O.; Smekens, J.; Coosemans, T.; Bossche, P.V.; et al. Lithium-ion capacitor–advanced technology for rechargeable energy storage systems. In Proceedings of the 2013 World Electric Vehicle Symposium and Exhibition (EVS27), Barcelona, Spain, 17–20 November 2013; pp. 1–11.
35. Fleurbaey, K.; Ronsmans, J.; Hoog, J.; Nikolian, A.; Timmermans, J.M.; Omar, N.; Bossche, P.V.; Mierlo, J.V. Lithium-ion capacitor - electrical and thermal characterization of advanced rechargeable energy storage component. In Proceedings of the European Electric Vehicle Congress 2014, Brussels, Belgium, 3–5 December 2014; pp. 1–11.
36. Campillo-Robles, J.M.; Artetxe, X.; Sánchez, K.D.T.; Gutiérrez, C.; Macicior, H.; Röser, S.; Wagner, R.; Winter, M. General hybrid asymmetric capacitor model: Validation with a commercial lithium ion capacitor. *J. Power Sources* **2019**, *425*, 110–120. [CrossRef]
37. Zhao, S.; Khan, N.; Nagarajan, S.; Trescases, O. Lithium-Ion-Capacitor-Based Distributed UPS Architecture for Reactive Power Mitigation and Phase Balancing in Datacenters. *IEEE Trans. Power Electron.* **2019**, *34*, 7381–7396. [CrossRef]
38. Miller, J.R. Engineering electrochemical capacitor applications. *J. Power Sources* **2016**, *326*, 726–735. [CrossRef]
39. Uno, M.; Kukita, A. Cycle life evaluation based on accelerated aging testing for lithium-ion capacitors as alternative to rechargeable batteries. *IEEE Trans. Ind. Electron.* **2016**, *63*, 1607–1617. [CrossRef]